

Thermodynamic diagnosis of a novel solar-biomass based multi-generation system including potable water and hydrogen production

ABSTRACT

Author

Nasim Hashemian^a
Alireza Noorpoor^{a*}
Parisa Heidarnejad^a

^a Graduate Faculty of
Environment, College of
Engineering, University of
Tehran, Tehran, Iran

In this study, a new proposed multi-generation system as a promising integrated energy conversion system is studied, and its performance is investigated thermodynamically. The system equipped with parabolic trough collectors and biomass combustor to generate electricity, heating and cooling loads, hydrogen and potable water. A double effect absorption chiller to provide cooling demand, a proton exchange membrane electrolyzer to split water into hydrogen and oxygen and a multi-effect desalination system to provide potable water by recovering the waste heat of biomass combustion is combined with a steam Rankine cycle. The results of the thermodynamic analysis indicate that thermal efficiency of 82.5% and exergy efficiency of 14.6% is achievable for the proposed system. Hydrogen and potable water production rates are 88.1 kg/h and 3.9 m³/h, respectively. The proposed system generates 26.3 MW electricity, 26.3 MW heating load, and 137.2 MW cooling load. Parabolic trough solar collector, double effect absorption chiller and biomass combustor are the primary sources of thermodynamic irreversibilities in comparison to other components. The mass flow rate of biomass fed to the system and aperture area of parabolic trough solar collector is calculated to be 6.2 ton/h and 188,000 m². Besides conventional analyses, to conclude the concept of multiplicity six different cases for the studied multi-generation system are modeled and evaluated regarding thermal and exergy efficiencies. Finally, the parametric study is performed to identify the consequential parameters on the thermodynamic performance of the system.

Article history:

Received : 26 May 2018
Accepted : 31 July 2018

Keywords: Exergy, Multi-Generation, Desalination, Hydrogen Production, Double Effect Absorption Chiller.

1. Introduction

Recently, using renewable energy sources as alternatives for fossil fuel sources is one of the appropriate solutions for current environmental problems. Multi-generation energy systems are a developed type of cogeneration systems which produces diverse products such as electricity, heating power, cooling power, synthesis fuel, potable water, materials, etc. Since the studied renewable based multi-generation system in this research has been

proposed for the Southern Region of Iran, biomass and solar energy are considered as the inputs of the system. The sufficient amount of as a type of biomass which is the corollary product in sugar industries [1] and solar radiation are available in this region (i.e, average of 5 kWh/m²/day) [2]. Lately, multiple types of research have been regarded to the evaluation of multi-generation systems with hydrogen production. Ahmadi et al. [3] presented thermodynamic modeling and multi-objective optimization of an ocean thermal energy based system for hydrogen production. To assess the role of key parameters such as solar radiation intensity and evaporator pinch

* Corresponding author: Alireza Noorpoor
Graduate Faculty of Environment, College of
Engineering, University of Tehran, Tehran, Iran
Email: Noorpoor@ut.ac.ir

point on system operation, sensitively analysis was performed. Exergy and energy efficiencies of a proposed multi-generation system including hydrogen production were estimated by Taheri et al. [4]. The largest exergy destruction rate occurred in combustion subsystem as they reported. They optimized the operation of this biomass and liquefied natural gas based multi-generation system from the thermodynamic point of view. Thermodynamic performance of a multi-generation energy system based on renewable energy was calculated by Akrami et al. [5]. The suggested a system for power, heating, cooling, and hydrogen production. According to their study, most exergy destruction rate occurred in the turbine. In another research, Sharifishourabi and Arab chadegani [6] designed a solar based multi-generation system for producing hydrogen energy. Thermodynamic performance of the system and effects of key parameters on efficiencies were conducted by authors. They concluded the proposed system can be used for residential buildings. Khanmohammadi et al. [7] provided a thermodynamic and thermoeconomic assessment of the multi-generation system to produce hydrogen energy. In order to determine the best system operation point, optimization was carried out from the thermodynamic and thermoeconomic points of view. Parham et al [8] assessed a system including freshwater and hydrogen by using the energy-exergy method. Moreover, the impacts of key parameters on system operation were demonstrated by authors. Boyaghchi et al. [9] examined a biomass-based multi-generation system with the purpose of generating syngas, power, cooling, heating, and hydrogen with different groups of working mediums. The optimum design of the system was determined based on thermodynamic, thermoeconomic and environmental criteria. Yuksel et al. [10] developed a geothermal-based multi-generation system for hydrogen production. Energy and exergy efficiencies were calculated 39.46% and 44.27%, respectively. the parametrical study showed the significance of some parameters on the thermodynamic performance of the system. A solar based system was modeled thermodynamically and thermoeconomically by Bellos et al. [11]. Also, the optimum performance of the system was determined by different performance criteria such as energy and exergy efficiencies and energy saving cash flow. The results of the financial study proved that the payback period of the studied is 3-4 years.

Water scarcity is another main concern of the current century because water consumption has been growing more than growth of the population in this century [12] which causes the dependence on water desalination. Whenever waste heat is available, Multi-Effect Desalination (MED) system is the distinguished desalination technology for production of potable water. The integration of MED systems into multi-generation systems has been taken into account by several researchers. Noorpoor et al. [13] applied energy and exergy methodology for a renewable-based multi-generation system for producing power, heating, cooling and potable water. They improved the thermodynamic performance of the proposed multi-generation system by multi-objective optimization. Calise et al. [14] presented a multi-generation energy system driven by solar energy. Power, heating, cooling and hot water produced as useful outputs. They found that required solar field area varies from 250-300 m². Moreover, they investigated effects of key parameters on the thermodynamic performance of system through sensitivity analysis. Mohammadi et al. [15] described energy and exergy methodology for the geothermal based multi-generation system to produce potable water. Also, the effects of key parameters on system performance were showed by the parametrical study. Recently, Javidmehr et al. [16] developed a renewable-based multi-generation system for producing fresh water. The results showed that solar collector and combustion chamber have a major contribution in for exergy destruction. In another research, a solar driven multi-generation system for producing fresh water was conducted by Rashidi and Khorshidi [17]. Sensitivity analysis was employed to show the effects of design parameters on thermodynamic efficiencies of the system. Ghasemi et al. [18] designed a new multi-generation system driven by biomass and solar energy for producing liquefied natural gas and fresh water. sensitivity analysis was conducted to show the effects of key parameters on system performance. Moreover, Multi-objective optimization applied to improve the system efficiency. Islam et al. [19] modeled a new solar-based multi-generation system to produce potable water. They utilized reverse osmosis unit for the desalination plant. Potable water demand of Off-Grid areas is met through the geothermal source. Moreover, Thermodynamic efficiencies of the system were examined by authors. Siddiqui and Dincer [20] assessed a new solar-based multi-generation system

through both energy and exergy approaches. Reverse osmosis was coupled to the system for sweet water production. Energy and exergy efficiencies were obtained 23.2% and 6.2%, respectively.

Based on the reviewed literature by authors, the present work has significant novelties compared to the existing studies as follows.

- A novel configuration of a multi-generation system is proposed to produce electricity, heating and cooling loads, hydrogen and potable water. Steam Rankine Cycle (SRC) is the core of the system which generates electricity and heating power. Double Effect Absorption Chiller (DEAC) is used for providing the cooling demand by consuming the waste heat of turbine. Hydrogen is generated by Proton Exchange Membrane (PEM) electrolyzer through separating water into hydrogen and oxygen, consuming a part of electricity. Multi Effect Desalination System (MED) is employed to produce potable water from the seawater utilizing the waste heat of biomass combustion.
- Solar and biomass energy are utilized as fuel simultaneously. Solar radiation is collected by Parabolic Trough Collector (PTC), and bagasse is combusted in biomass combustor.
- Thermodynamic assessment including energy and exergy analysis of each component and the overall system is carried out to determine the thermodynamic performance of the system. Exergy destruction rate of the system is calculated to identify the sources of inefficiencies.
- With the goal of comprehension about the consequences of integrating different subsystems, different cases of the multi-generation system are compared regarding thermal and exergy efficiencies.

Finally, the effect of essential design parameters on the thermal and exergy efficiencies of the proposed system and cooling output, heating output, direct use electricity and potable water production by the system is discussed by performing sensitivity analysis.

Nomenclature

A	area, m ²
BC	biomass combustor
DEAC	double effect absorption chiller
Ex	Exergy rate, MW
F	Faraday constant, C/mol

G	Gibbs free energy, kJ
G _t	total instantaneous radiation, W/ m ²
H	total enthalpy, kW
h	specific enthalpy, kJ/kg
J ^{ref}	pre-exponential factor, A/ m ²
J ₀	exchange current density, A/ m ²
J	Current Density, A/ m ²
L	membrane thickness, m
HHV	Higher heating value, kJ/kg
m [·]	mass flow rate, kg/s
multi	multi-generation system
P	pressure, kPa
PEM	Proton exchange membrane
R _{PEM}	proton exchange membrane resistance, Ω
R	gas constant, kJ/kg K
s	specific entropy, kJ/kg K
T	temperature, K
V _{act}	activation overpotential, V
V ₀	reversible potential, V
V _{act,a}	anode activation overpotential, V
V _{act,c}	cathode activation overpotential, V
V _{ohm}	ohmic overpotential, V
\dot{W}	power, W

Greek letters

η	thermal efficiency
ε	exergy efficiency
λ	water content in ionomer
σ	proton conductivity in PEM, 1/ Ω m

Subscripts

0	reference environment state
eva	Evaporator

Abbreviations

CCHP	Combined Cooling Heating and Power
COP	Coefficient of Performance
EES	Engineering Equation Solver
HHV	High Heating Value
HHX	High-temperature heat exchanger
HTG	High-temperature generator
LTG	Low-temperature generator
LHX	Low-temperature heat exchanger
MED	Multi Effect Desalination
Multi	Multi-generation energy system
ORC	Organic Rankine Cycle
PEM	Proton Exchange Membrane
SG	Single Generation
SRC	Steam Rankine Cycle

2. Material and methods

2.1. The studied multi-generation system

Figure 1 shows the proposed multi-generation energy system including parabolic trough solar collectors (PTC), a biomass combustor (BC), a steam Rankine cycle (SRC), a double effect absorption chiller (DEAC), a proton exchange membrane (PEM) electrolyzer and a multi-effect desalination system (MED). Outputs of the proposed system are electricity, heating, cooling, hydrogen and potable water. Inputs are solar energy and bagasse as biomass. Solar energy is exploited through PTC, and the type of collector applied in this system is SL3 [21]. Since Therminol VP-1 oil has good heat transfer properties and stability at high temperature [22], it is selected as working fluid of solar collector. The temperature of Therminol VP-1 is raised by absorbing the solar radiation which acts as an intermittent energy source. For neutralizing the inconsistency, a biomass combustor is applied, and as a result, the total energy requirement of the system is supplied. In the SRC subsystem,

the heat released from biomass combustor is consumed to produce superheated steam (point 4) for generating power in the turbine (point 25). The fluid after the turbine is used by HX1 to provide the heating load. In DEAC subsystem, by the heat of the outlet steam of the HX1, the refrigerant (H₂O) and the absorbent (LiBr) is separated. The H₂O is condensed in the condenser and enters the evaporator 2 to provide the cooling load after its pressure drops down in valve4. In absorber, the outlet steam of evaporator 2 is absorbed by the H₂O-LiBr coming from LHX and is pumped into LHX, HHX, and HTG respectively. Another capability of this system is producing potable water by MED. Hot exhaust gasses of bagasse combustion enter the HX2 (point 10) to prepare the required energy for the thermal desalination system. In each effect, pure water is produced at upper pressure and lower temperature than the next effect. The produced vapor of each effect acts as the heating steam for the following effect which makes the MED as a promising technology when an amount of waste heat is available.

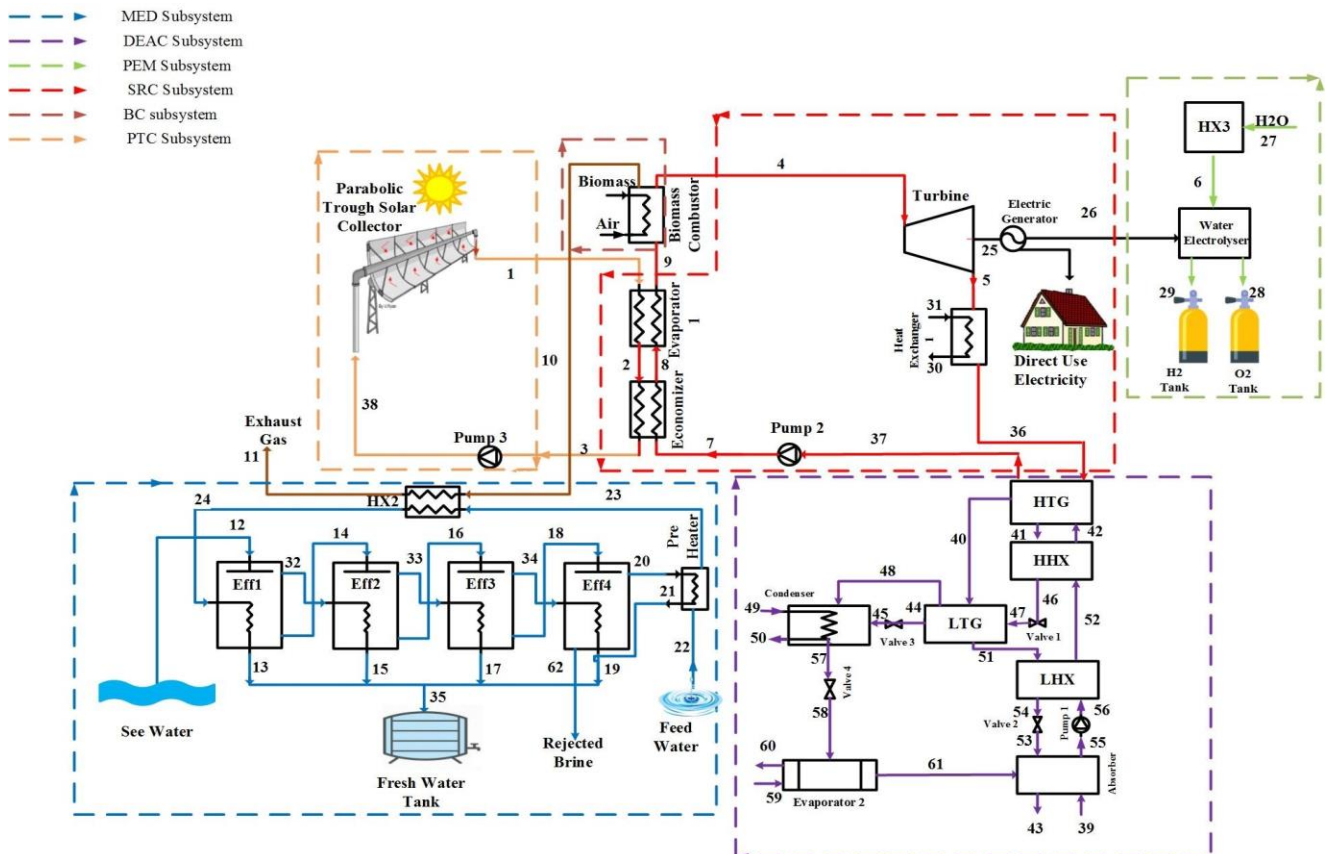


Fig. 1. Schematics of the proposed integrated energy system

Finally, a portion of electricity production by the turbine and electric generator is consumed in the PEM electrolyzer to produce hydrogen. Heated water is fed to electrolyzer (point 6) separated to hydrogen by the cathode and oxygen by the anode through electrolysis reaction. The produced hydrogen is stored in the storage tank for further usage.

2.2. Energy Analysis

To better understand the energetic performance of the proposed multi-generation energy system, thermodynamic modeling of each subsystem is presented based on the mass balance and the first law of thermodynamics:

2.2.1. Steam Rankine Cycle (SRC) Subsystem

SRC subsystem includes an evaporator1, an economizer, a turbine, a heat exchanger1 and a pump2. Power and heating are generated in this subsystem by turbine and heat exchanger1. Evaporator1 and economizer are employed to provide steam which is used to drive turbine and heat exchanger1. Energy rate balance for each element of this subsystem can be written as follows:

Evaporator1:

$$\dot{m}_1(h_1 - h_2) = \dot{m}_8(h_9 - h_8) \quad (1)$$

Turbine:

$$\dot{W}_{turb} = \dot{m}_4(h_4 - h_5) \quad (2)$$

$$\eta_{is,turb} = \frac{\dot{W}_{turb}}{\dot{W}_{is,turb}} \quad (3)$$

Heat exchanger1:

$$\dot{E}_{heating} = \dot{m}_5(h_5 - h_{36}) \quad (4)$$

Pump2:

$$\dot{W}_{pump2} = \dot{m}_{37}v_{37}(p_7 - p_{37})/\eta_{is,pump} \quad (5)$$

Economizer:

$$\dot{m}_3(h_2 - h_3) = \dot{m}_8(h_8 - h_7) \quad (6)$$

2.2.2. Parabolic Trough Collector (PTC) Subsystem

Solar radiation is collected by PTC to provide required input energy of the system. Governing

equation of PTC subsystem can be written as follows [23, 24]:

$$\dot{E}_s = \dot{m}_{38}C_p(T_1 - T_{38}) \quad (7)$$

Here, C_p is specific heat for Thermion VP-1 oil.

$$\dot{E}_s = A_a F_R \left(S - \frac{A_r}{A_a} U_L (T_{38} - T_0) \right) \quad (8)$$

Here, F_R is the heat removal factor, S is the heat absorbed by the receiver, A_r and A_a are the receiver and aperture areas, and U_L is the solar collector overall heat loss coefficient.

2.2.3. Biomass Combustor Subsystem

To supply input energy, when the solar radiation is not sufficient during nights and cloudy days, biomass combustor is employed to compensate for the shortage of solar radiation. In this subsystem, excess air and bagasse as biomass enter biomass combustor, and combustion occurs. The energy balance of biomass can be expressed as:

$$\eta_{BC} \times (\dot{m}_{bio} HHV_{bio} + \dot{m}_{air} h_{air}) = \quad (9)$$

$$\dot{m}_4(h_4 - h_9) + \dot{m}_{10}h_{10}$$

$$\dot{E}_{BC} = \dot{m}_{bio} HHV_{bio} \quad (10)$$

where HHV of bagasse is taken to be 17000 kJ/kg [25] and η_{BC} is biomass combustor efficiency.

2.2.4. Double Effect Absorption Chiller (DEAC) Subsystem

This subsystem includes two generators, namely: low-temperature generator (LTG) and high-temperature generator (HTG), a pump, an absorber, an evaporator (evaporator2), a condenser and two heat exchangers, namely: high heat exchanger (HHX) and low heat exchanger (LHX). Water is used as refrigerant and lithium bromide is used as an absorbent. In the evaporator2, cooling power is generated by cooled water which can be used for space cooling. Energy balances for components of this subsystem can be written as follows:

Evaporator2:

$$\dot{E}_{cooling} = \dot{m}_{61}(h_{61} - h_{58}) \quad (11)$$

HTG:

$$\dot{Q}_{HTG} + \dot{m}_{42}h_{42} = \dot{m}_{40}h_{40} + \dot{m}_{41}h_{41} \quad (12)$$

$$\dot{m}_{41}x_{41} = \dot{m}_{42}x_{42} \quad (13)$$

LTG:

$$\dot{m}_{40}(h_{40} - h_{44}) = \quad (14)$$

$$\dot{m}_{48}h_{48} + \dot{m}_{51}h_{51} - \dot{m}_{47}h_{47}$$

$$\dot{m}_{47}x_{47} = \dot{m}_{51}x_{51} \quad (15)$$

HHX:

$$\dot{m}_{42}h_{42} - \dot{m}_{52}h_{52} = \dot{m}_{41}h_{41} - \dot{m}_{46}h_{46} \quad (16)$$

LHX:

$$\dot{m}_{51}h_{51} - \dot{m}_{54}h_{54} = \dot{m}_{52}h_{52} - \dot{m}_{56}h_{56} \quad (17)$$

Absorber:

$$\dot{Q}_{ABS} + \dot{m}_{55}h_{55} = \dot{m}_{61}h_{61} + \dot{m}_{53}h_{53} \quad (18)$$

$$\dot{m}_{55}x_{55} = \dot{m}_{53}x_{53} \quad (19)$$

Condenser:

$$\dot{Q}_{cond} + \dot{m}_{57}h_{57} = \dot{m}_{45}h_{45} + \dot{m}_{48}h_{48} \quad (20)$$

2.2.5. Proton Exchange Membrane Electrolyzer (PEM) Subsystem

In this subsystem, heat and electricity are fed to the electrolyzer to drive the electrochemical reaction. Water is entered to Heat exchanger3 (HX3) to reach the temperature of PEM and then goes to the electrolyzer. During electrolysis process, oxygen produced in the anode and hydrogen produced in the cathode of PEM electrolyzer and both of them cooled down to ambient condition. Turbine supplies the electric power required for electrochemical reaction. The energy needed for PEM electrolyzer subsystem can be estimated as follows [26]:

$$\Delta H = \Delta G + T\Delta S \quad (21)$$

where ΔG is Gibb's free energy and $T\Delta S$ is thermal energy demand.

$$\dot{E}_{26} = JV \quad (22)$$

$$V = V_0 + V_{act,a} + V_{act,c} + V_{ohm} \quad (23)$$

Here V is PEM electrolyzer voltage, V_0 is the reversible potential that is determined by Nernst equation, $V_{act,a}$ and $V_{act,c}$ are activation overpotential of the anode and cathode, and V_{ohm} is ohmic overpotential of the electrolyte [27]:

$$\delta[\lambda(x)] = [0.5139\lambda(x) - 0.326] \quad (24)$$

$$\exp[1268(\frac{1}{303} - \frac{1}{T})]$$

Here, $\sigma(x)$ is local ionic conductivity of the PEM, x is the depth in the membrane, and $\lambda(x)$ is the water content at location x [28]:

$$\lambda(x) = \frac{\lambda_a - \lambda_c}{D_L}x + \lambda_c \quad (25)$$

Here, D is the membrane thickness; λ_a and λ_c are the water contents at the anode and the cathode-membrane interface [28]:

$$R_{PEM} = \int_0^L \frac{dx}{\delta[\lambda(x)]} \quad (26)$$

where R_{PEM} is overall ohmic resistance.

$$\eta_{ohm} = JR_{PEM} \quad (27)$$

Here, η_{ohm} is ohmic overpotential.

$$J = J_{o,i} [\exp(\frac{\alpha ZF\lambda_{act,i}}{RT}) - \exp(\frac{(\alpha-1)ZF\lambda_{act,i}}{RT})], i = a, c \quad (28)$$

Here, J is activation overpotential that can be defined by Butler-Volmer equation. $J_{o,i}$ is the exchange current density, α is the symmetrical factor, z is the number of electrons involved per reaction. For water electrolysis, α and z are found to be 0.5 and 2 respectively [29]:

$$\lambda_{act,i} = \frac{RT}{F} \sinh^{-1}(\frac{J}{2J_{o,i}}), i = a, c \quad (29)$$

Here, $\lambda_{act,i}$ is activation overpotential of an electrode. [29]

$$J_{o,i} = J_i^{ref} \exp(-\frac{V_{act,i}}{RT}), i = a, c \quad (30)$$

here, J_i^{ref} is the pre-exponential factor and $V_{act,i}$ is the activation energy for the anode and cathode.

2.2.6. Multi Effect Desalination (MED) Subsystem

This subsystem includes a heat exchanger (HX2), a preheater and four effects for the process of evaporating and condensing. After feed water passes through preheater enters into HX2 and its temperature rises. Steam generated through the flash process in each effect has lower pressure and temperature than the previous effect which causes the evaporation implemented independently of any external energy source in each effect except to

effect 1. Governing equation of MED subsystem can be written as follows:

$$\dot{m}_{35} = \dot{m}_{13} + \dot{m}_{15} + \dot{m}_{17} + \dot{m}_{19} + \dot{m}_{21} \quad (31)$$

$$\dot{m}_{35} + \dot{m}_{62} = \dot{m}_{22} + \dot{m}_{12} \quad (32)$$

$$\dot{E}_{MED} = \dot{m}_{12}(h_{35} - h_{12}) \quad (33)$$

$$\dot{E}x_Q = \dot{Q}(1 - \frac{T_0}{T}) \quad (35)$$

$$\dot{E}x_W = \dot{W} \quad (36)$$

$$ex = (h - h_0) - T_0(s - s_0) \quad (37)$$

2.3. Exergy Analysis

Exergy analysis is an applicable tool which provides comprehensive information about the reasons and locations of inefficiencies of the energy system which is employed by applying exergy balance to all components of the system. Exergy destruction rates and exergy efficiencies for elements of the multi-generation system based on the below exergy balance are listed in Table 1.

$$\dot{E}x_D = \sum \dot{E}x_Q - \sum \dot{E}x_W + \sum_i \dot{m}_i ex_i - \sum_e \dot{m}_e ex_e \quad (34)$$

2.4. Thermal and Exergy Efficiencies of the system

Assessment of thermal efficiency is the main part of the process of energy management which represents the first step in analyzing the energy systems. The thermal efficiency of the multi-generation is formulated as below:

$$\eta_{multi} = \frac{\dot{W}_{direct-use} + \dot{E}_{cooling} + \dot{E}_{heating} + \dot{E}_{MED} + \dot{E}_{PEM}}{\dot{E}_{BC} + \dot{E}_s} \quad (38)$$

Table 1. Exergy destruction rate and exergy efficiency of system components

Components	Exergy Destruction Rate	Exergy Efficiency
PTC	$\dot{E}x_{D,PTC} = \dot{E}x_s - \dot{m}_1(ex_1 - ex_{38})$	$1 - \frac{\dot{E}x_{D,PTC}}{\dot{E}x_s}$
Evaporator1	$\dot{E}x_{D,Eva1} = \dot{m}_1(ex_1 - ex_2) - \dot{m}_8(ex_9 - ex_8)$	$1 - \frac{\dot{E}x_{D,Eva1}}{\dot{m}_1(ex_1 - ex_2)}$
Pump2	$\dot{E}x_{D,pump2} = \dot{W}_{pump2} - \dot{m}_{37}(ex_7 - ex_{37})$	$1 - \frac{\dot{E}x_{D,pump2}}{\dot{W}_{pump2}}$
Heat Exchanger1	$\dot{E}x_{D,HX1} = \dot{m}_5(ex_5 - ex_{36}) - \dot{m}_{31}(ex_{30} - ex_{31})$	$1 - \frac{\dot{E}x_{D,HX1}}{\dot{m}_5(ex_5 - ex_{36})}$
Turbine	$\dot{E}x_{D,turb} = \dot{m}_4(ex_4 - ex_5) - \dot{W}_{turb}$	$1 - \frac{\dot{E}x_{D,turb}}{\dot{m}_4(ex_4 - ex_5)}$
Electrolyzer	$\dot{E}x_{D,PEM} = ex_{26} + \dot{m}_{27}(ex_6 - ex_{27}) - (ex_{29} + ex_{28})$	$1 - \frac{\dot{E}x_{D,PEM}}{ex_{26} + \dot{m}_{27}(ex_6 - ex_{27})}$
Biomass combustor	$\dot{E}x_{D,BC} = \dot{E}x_{bio} + \dot{m}_{air}ex_{air} - \dot{m}_{10}ex_{10} - \dot{m}_4(ex_4 - ex_9)$	$1 - \frac{\dot{E}x_{D,BC}}{\dot{E}x_{bio} + \dot{m}_{air}ex_{air} - \dot{m}_{10}ex_{10}}$
MED	$\dot{E}x_{D,MED} = \dot{m}_{10}(ex_{10} - ex_{11}) - (\dot{m}_{35}ex_{35} - \dot{m}_{12}ex_{12} - \dot{m}_{22}ex_{22}) - \dot{m}_{62}ex_{62}$	$1 - \frac{\dot{E}x_{D,MED}}{\dot{m}_{10}(ex_{10} - ex_{11})}$
DEAC	$\dot{E}x_{D,DEAC} = \dot{m}_{36}(ex_{36} - ex_{37}) + \dot{m}_{49}(ex_{49} - ex_{50}) + \dot{m}_{39}(ex_{39} - ex_{40}) - \dot{m}_{59}(ex_{60} - ex_{59})$	$1 - \frac{\dot{E}x_{D,DEAC}}{\dot{m}_{36}(ex_{36} - ex_{37})}$

$$\dot{E}_{PEM} = \dot{m}_{29} HHV_{H_2} \quad (39)$$

$$\begin{aligned} \dot{W}_{direct-use} &= \dot{W}_{turb} \eta_{EG} - \dot{W}_{pump1} - \\ &\dot{W}_{pump2} - \dot{W}_{pump3} - \dot{E}_{26} \end{aligned} \quad (40)$$

The items involved in the thermal efficiency of the system were explained in the previous sections.

The equivalent exergy outputs of the multi-generation system are electricity for direct use ($\dot{W}_{direct-use}$), exergy of cooling power ($\dot{E}x_{cooling}$), exergy of heating power ($\dot{E}x_{heating}$), exergy amount associated to water desalination ($\dot{E}x_{MED}$) and exergy content of produced hydrogen ($\dot{E}x_{PEM}$). The exergy inputs of the system are the exergy from solar radiation ($\dot{E}x_s$) and exergy resulted from bagasse combustion ($\dot{E}x_{BC}$). The exergy efficiency of the multi-generation is calculated as:

$$\varepsilon_{multi} = \frac{\dot{W}_{direct-use} + \dot{E}x_{cooling} + \dot{E}x_{heating} + \dot{E}x_{MED} + \dot{E}x_{PEM}}{\dot{E}x_{BC} + \dot{E}x_s} \quad (41)$$

$$\dot{E}x_{cooling} = \dot{m}_{59}(ex_{60} - ex_{59}) \quad (42)$$

$$\dot{E}x_{heating} = \dot{m}_{30}(ex_{30} - ex_{31}) \quad (43)$$

$$\dot{E}x_{MED} = \dot{m}_{12}(ex_{35} - ex_{12}) \quad (44)$$

$$\dot{E}x_{PEM} = \dot{m}_{29} ex_{H_2}^{ch} \quad (45)$$

$$\dot{E}x_{BC} = \dot{m}_{bio} ex_{bio}^{ch} \quad (46)$$

$$\begin{aligned} \dot{E}x_s &= A_{coll} \times G_t \times \\ &\left[1 + \frac{1}{3} \left(\frac{T_0}{T_s} \right)^4 - \frac{4}{3} \left(\frac{T_0}{T_s} \right) \right] \end{aligned} \quad (47)$$

The coefficient of performance for the double effect absorption chiller is defined as the ratio of cooling load provided by chiller to the received heat through high-temperature generator and work consumed by solution pump as follows:

$$COP_{th} = \frac{\dot{E}x_{cooling}}{\dot{Q}_{HTG} + \dot{W}_{pump1}} \quad (48)$$

Exergetic Coefficient of Performance is the most common parameters of the absorption system performance and is defined as the ratio of exergy of cooling load provided by chiller to the received exergy through high-temperature generator and work consumed by solution pump as follows:

$$COP_{ex} = \frac{\dot{E}x_{cooling}}{\dot{E}x_{HTG} + \dot{W}_{pump1}} \quad (49)$$

3. Model validation

3.1. PEM electrolyzer

In order to validate the result of PEM electrolyzer subsystem, the present study is compared with the experimental data given in [30]. Figure 2 Shows the slight differences between the effect of current density, J , and cell potential, V , in two works.

3.2. MED Subsystem

To verify the MED subsystem modeling, Distillate Production and temperature difference have been compared with the result, which has been obtained by Ghasemi et al. [18]. Table 2 shows the reasonable difference between the current work and a previous study.

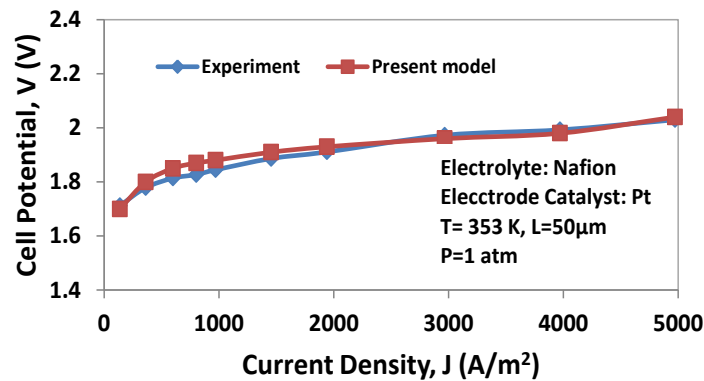


Fig.3. Impact of the cell potential value on current density in present model and experimental study [30]

Table 2. Comparison of current study result with the result of Ghasemi et al.[18]

Parameters	Current study	Ref [18]
Mass flow rate ratio of potable water to seawater	2.1	2.23
Mass flow rate ratio of potable water to motive steam	1.4	1.58
Mass flow rate ratio of potable water to exhaust gasses of biomass burner	0.62	0.71

4. Results and Discussion

The studied multi-generation system consumes solar energy and energy of bagasse combustion as energy sources to provide electricity, cooling power, heating power, hydrogen and potable water. This system is proposed for a coastal area of the southern region of Iran since the solar radiation is the considerable and adequate amount of bagasse (approximately 1,200,000 ton/year [31]) is produced in this region. The average solar daily radiation on a horizontal surface is extracted from NASA online database [30]. The calculations are conducted by formulating first and second laws of thermodynamics and solving the equations by using EES (Engineering Equation Solver) software [32]. For simplifying the thermodynamic modeling of the multi-generation system, following assumptions are considered:

- The ambient temperature and pressure are $T_0 = 298$ K, $P_0 = 100$ kPa.
- The seawater salinity is 40 g/kg.
- The MED has four effects.
- The system operates under the steady state conditions. The system has negligible changes in kinetic, and potential energy and exergy.
- The sun temperature is $T_s = 6000$ k.
- Working fluid of double effect absorption chiller is a solution of LiBr/H₂O.

- Higher heating value (HHV) is approximately equal to chemical exergy of biomass [33], and efficiency of biomass combustor is 80%.

In Table 3 input data parameters for thermodynamic modeling of the system are shown.

Table 4 summarizes the performance specifications of the multi-generation system such as total electricity, electricity consumed by electrolyzer, electricity for direct use, cooling power, heating power, the amount of hydrogen production, the amount of potable water production, required aperture area of the solar collector, required mass flow rate of bagasse, energetic and exergetic COP, thermal and exergy efficiencies of the multi-generation system.

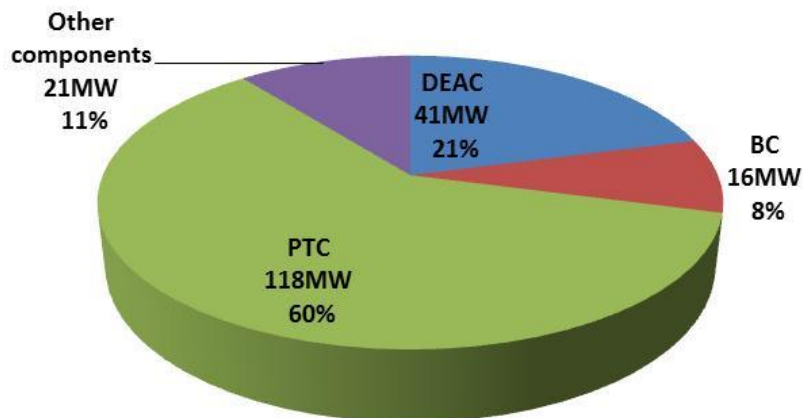
Figure 3 shows the exergy destruction rates of each component of the multi-generation system. As presented in Figure 3, PTC unit is responsible for 60% of exergy destruction rate of the multi-generation system. Because of the temperature difference between the receivers and the Therminol VP-1, major exergy destruction rates contributor is PTC. Since the temperature difference between the solution of LiBr-H₂O and vapor passes through the components results irreversibilities, DEAC is the second highest inefficient subsystem. In BC as the third inefficient subsystem, the irreversibility

Table 3. Input data for thermodynamic modeling

Parameter	Value
Turbine inlet temperature (°C)	550
Turbine inlet pressure (kPa)	6000
Turbine pressure ratio	45
Heat exchanger1 temperature difference (°C)	10
The temperature difference between each effect of MED(°C)	5
The pressure difference between each effect of MED (kPa)	0.3
Turbine isentropic efficiency	0.85
Pumps isentropic efficiency	0.7
Hydrogen High Heating Value (MJ/kg)	141.88
Area of solar collector (m ²)	188,000

Table 4. Thermodynamic performance of the multi-generation system

Parameter	Value
Total electricity output (MW)	31.3
Direct use of electricity (MW)	26.3
Electricity to electrolyzer (MW)	5
Cooling power (MW)	137.2
Heating power (MW)	21.4
Hydrogen production (kg/h)	88.1
Potable water production (m ³ /h)	3.9
The mass flow rate of bagasse (ton/h)	6.2
Exergetic COP (-)	0.19
Energetic COP (-)	1.63
Solar fraction (%)	88
Thermal efficiency (%)	82.5
Exergy efficiency (%)	14.6

**Fig.3.** Exergy destruction rates of the components

occurs as the result of combustion of biomass. Discussed subsystems are the main contributors to the overall exergy destruction rates of the system, and they have the main potential for improvement of the performance of the system to achieve a more efficient system.

Figure 4 illustrates the benefits of the multiplicity of useful outputs concerning energy and exergy efficiencies. Six cases such as Single Generation (SG), Combined Heat and Power (CHP), Combined Cooling Heating and Power (CCHP), Multi-generation including PEM (Multi(PEM)), Multi-generation including MED (Multi(MED)) and, Multi-generation including PEM and MED (Multi(MED-PEM)) are selected and analyzed in order to emphasise the advantages of the

cogeneration systems. In all cases, the amounts of energy and exergy inputs are similar to make an accurate comparison. As it is evident in Figure 4, by adding one more product to the single generation system, the thermal efficiency improves 10% while by adding two more products (cooling and heating) to it, the thermal efficiency increases about 70% due to the significant amount of cooling output produced by DEAC. Since 16% of electrical power is fed to PEM for hydrogen production which is wasted in the process of hydrogen production and results in the drop of thermal efficiency to about 24%. The reason of increment of the thermal efficiency in the case of adding potable water as an output to CCHP system is, utilizing the waste heat of the system to produce one more useful product. As it is

seen in the case of a Multi (MED-PEM) system, the thermal efficiency is lower than Multi (MED) case. The reason is apparently the same for Multi (PEM) as well. About exergy efficiency, by combining a heat exchanger to a single generation cycle to generate heating power, the exergy efficiency grows up to about 15.13%. In the CCHP case, exergy efficiency increases about 1.5% in comparison to CHP case as a result of generating cooling exergy through the DEAC by using the waste heat of the cycle. By integrating PEM to a CCHP system, 16% of electric power generated by the electric generator is consumed by electrolyzer, and a portion of it is devalued during the process of electrolyzing the water. Hence, the exergy efficiency is 2% lower than the CCHP case. On the other hand, the exergy efficiency in the Multi (MED) case is 0.05% more than CCHP case because the exergy produced by MED subsystem is not considerable. Since the process of hydrogen production is one of the main destructors, Multi (PEM) and Multi (MED-PEM) cases are less efficient than CCHP case. It is noted that, if the variety of products is not essential and the aim is improving the thermal and exergy efficiencies, integrating the MED subsystem to the cycle is an appropriate option.

4.1.Sensitivity Analysis

In this section, the effect of design parameters on the performances of the multi-generation system is investigated and discussed. The most effective parameters are selected to be turbine inlet pressure (P_4), inlet quality of high-temperature generator (q_{36}), the evaporator2

temperature (T_{eva2}) and the temperature difference of evaporator1 (ΔT_{eva1}).

4.1.1. Effect of turbine inlet pressure on the thermal and exergy efficiencies of the multi-generation system

Figure 5 illustrates the effect of turbine inlet pressure on thermal and exergy efficiencies of the system. By increasing turbine inlet pressure from 6000 kPa to 7000 kPa, the thermal efficiency of the multi-generation system improves by 5% because the useful energy output of the system increases. By variation of turbine inlet pressure, exergy efficiency of the multi-generation system grows about 1.2% due to the increment of the useful exergy output of the system. Note that higher the turbine inlet pressure higher will be the amount of electric power and amount of energy and exergy generating by HX1 and DEAC.

4.1.2. Effect of inlet quality of high-temperature generator on the thermal and exergy efficiencies of the multi-generation system

Figure 6 presents the relation of inlet quality of high-temperature generator and thermal and exergy efficiencies of the multi-generation system. By increasing the inlet quality from 0.2 to 0.9, the thermal efficiency of the system improves about 20%, because of the amount of energy feeding to DEAC increases and the amount of energy feeding to HX1 decreases, but the increment is dominant to decrement. By the variation of inlet quality of high-temperature generator, exergy efficiency drops down from 17.91% to 14.01%.

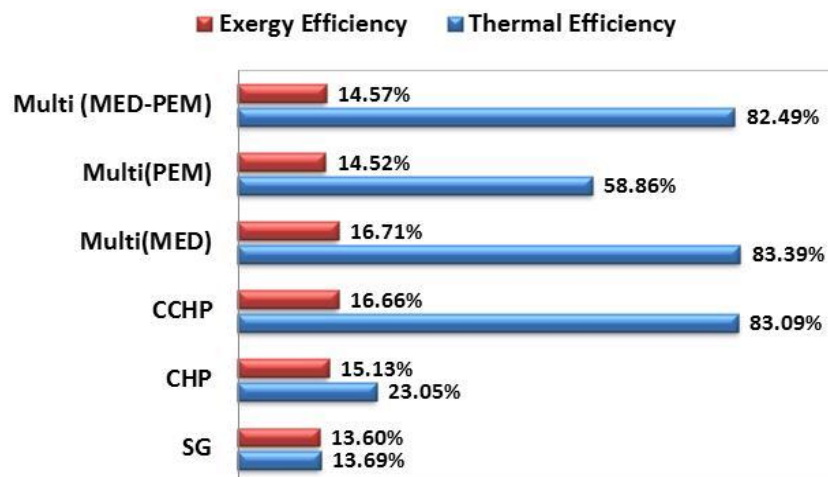


Fig.4. Advantages of cogeneration system regarding thermal and exergy efficiencies

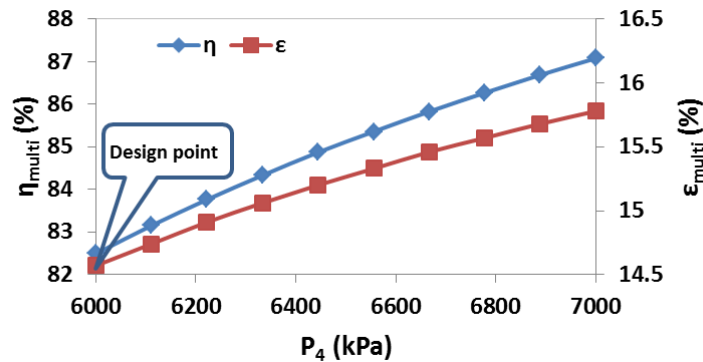


Fig.5. Effect of turbine inlet pressure on thermal and exergy efficiencies of the multi-generation system ($q_{36}=0.8$, $T_{\text{eva}2}=10^\circ\text{C}$, $\Delta T_{\text{eva}1}=10^\circ\text{C}$)

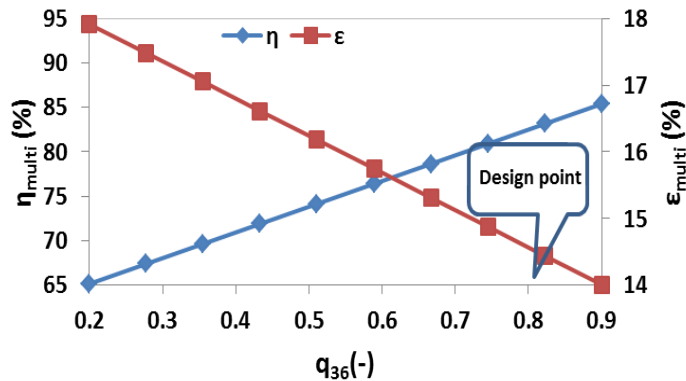


Fig. 6. Effect of inlet quality of high-temperature generator on thermal and exergy efficiencies of the multi-generation system ($P_4=6000\text{kPa}$, $T_{\text{eva}2}=10^\circ\text{C}$, $\Delta T_{\text{eva}1}=10^\circ\text{C}$)

When inlet quality of high-temperature generator increases, the amount of exergy feeding to DEAC increases and the amount of exergy feeding to HX1 decreases, but in this case, the decrement is dominant to increment.

4.1.3. Effect of evaporator2 temperature on the thermal and exergy efficiency of the multi-generation system

The relation of the evaporator2 temperature and the thermal and exergy efficiencies of the multi-generation system is indicated in Fig. 7. The increment of the temperature of evaporator2 results in an improvement in thermal efficiency because of the cooling amount generating by DEAC increases. On the other hand, rising the evaporator2 temperature leads to the decrement of the amount of exergy containing in cooling output. Hence exergy efficiency drops down from 16.72% to 13.54%.

4.1.4. Effect of temperature difference of evaporator1 on the thermal and exergy efficiency of the multi-generation system

The influence of temperature difference of evaporator1 on thermal and exergy efficiencies of the multi-generation system is presented in Fig.8. It is obvious that by increasing the temperature difference of evaporator1 from 10°C to 20°C , both thermal and exergy efficiencies improve. The temperature difference of evaporator1 followed by inlet temperature of biomass combustor (state 9) has the critical role in determining the mass flow rate of working fluid of steam Rankine cycle. Higher temperature difference requires higher mass flow rate and as a result the amount of energy and exergy feeding to turbine increases. Therefore, thermal and exergy efficiencies improve about 3% and 1% respectively.

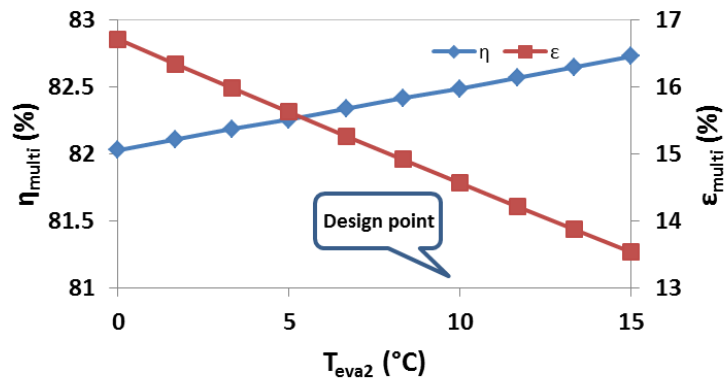


Fig.7. Effect of evaporator2 temperature on thermal and exergy efficiencies of the multi-generation system ($P_4=6000\text{kPa}$, $q_{36}=0.8$, $\Delta T_{eva1}=10^\circ\text{C}$)

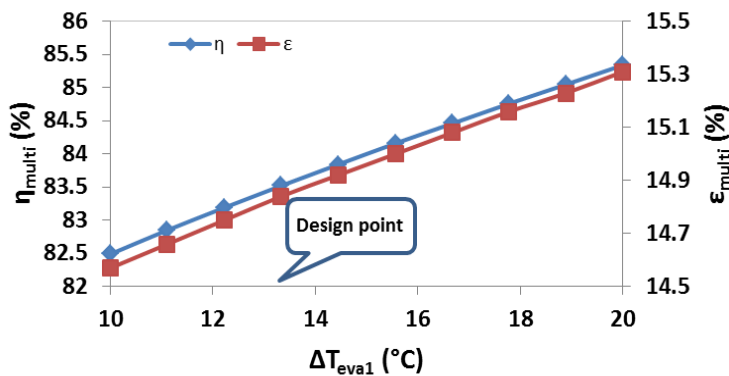


Fig.8. Effect of temperature difference of evaporator1 on thermal and exergy efficiencies of the multi-generation system ($P_4=6000\text{kPa}$, $q_{[36]}=0.8$, $T_{eva2}=10^\circ\text{C}$)

4.1.5. Effect of turbine inlet pressure on cooling output, heating output, direct-use electricity and potable water production of the multi-generation system

pressure on cooling and heating outputs of the multi-generation system. The enthalpy of the stream entering the turbine increases by increasing the turbine inlet pressure and as a result more heating and cooling outputs are provided.

Figure 9 illustrates the effect of turbine inlet

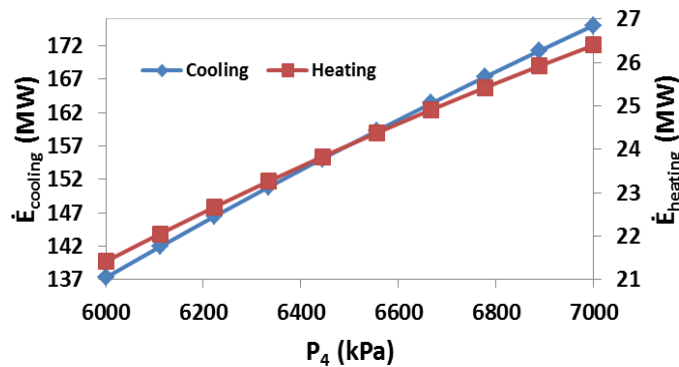


Fig.9. Effect of varying turbine inlet pressure on cooling and heating outputs of the multi-generation system

an increase in the turbine inlet pressure causes to more electricity generation by the system for the same reason for Fig.8 which is presented in Fig.10. The mass flow rate of the exhaust gasses of biomass combustion increases by an increase in turbine inlet pressure. Hence, the amount of potable water production increases.

4.1.6. Effect of temperature difference of evaporator1 on cooling output, heating output, direct-use electricity and freshwater production of the multi-generation system

Figure 11 shows the effect of varying temperature difference of evaporator1 on cooling and heating outputs of the multi-generation system. Both cooling and heating outputs of the multi-generation system are

observed to increase with increasing the temperature difference of evaporator1. When the temperature difference of evaporator1 increases, the mass flow rate of the steam Rankine cycle increases based on an energy balance across the control volume around evaporator1. The increment in the mass flow rate leads to more heating and cooling loads production.

Figure 12 shows the effect of temperature difference of evaporator1 on direct-use electricity and potable water production. By increasing the mass flow rate of steam Rankine cycle as a result of increment of temperature difference, the amount of electricity produced by the system increases. On the other hand, the mass flow rate of exhaust gasses of biomass combustion increases by this variation and leads to more production of potable water.

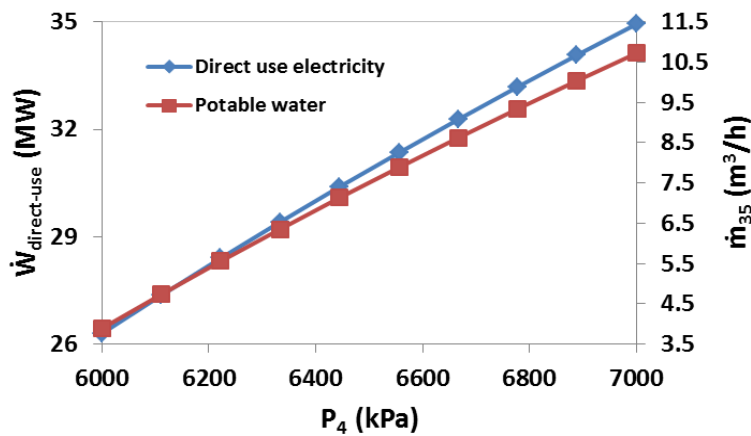


Fig.10. Effect of varying turbine inlet pressure on direct-use electricity and potable water production by the multi-generation system

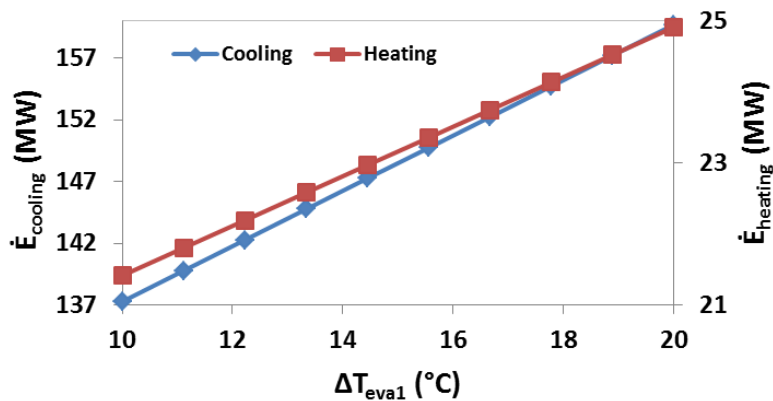


Fig.11. Effect of varying temperature difference of evaporator1 on cooling and heating outputs of the multi-generation system

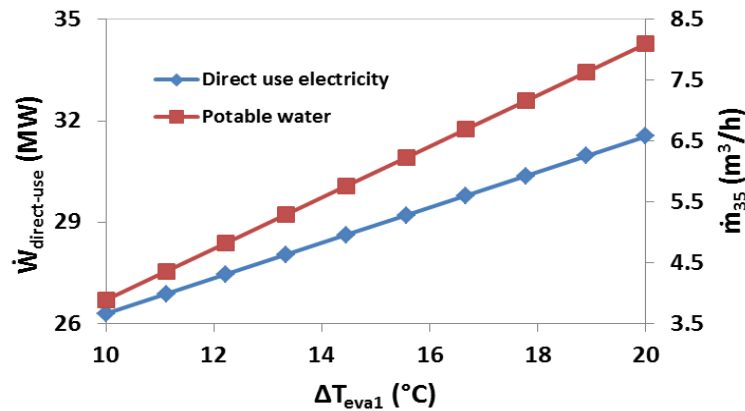


Fig.12. Effect of varying temperature difference of evaporator1 on direct-use electricity and potable water production by the multi-generation system

4.1.7. Effect of temperature difference of evaporator1 and turbine inlet pressure on thermal and exergy efficiencies of the different cases of multi-generation systems

In Fig.13a, the increment of temperature difference of evaporator1 causes an increase in the working fluid mass flow rate in steam Rankine cycle. Hence, improves the thermal efficiencies of all cases. In Fig.13b, by increasing the inlet pressure of turbine from 6000kPa to 7000kPa, more energy is provided

to turbine, and as a result, more electricity output is provided which leads to variation of the thermal efficiency of SG, CHP, CCHP, Multi(MED), Multi (PEM), Multi (MED-PEM) ascendingly. Figure 13c shows that when the temperature difference of evaporator1 increases from 10°C to 20°C, exergy efficiencies for all six cases improves due to the increment of working fluid mass flow rate in steam Rankine cycle. When turbine inlet pressure varies between 6000kPa and 7000kPa in Fig.13d, the exergy fed to the turbine is

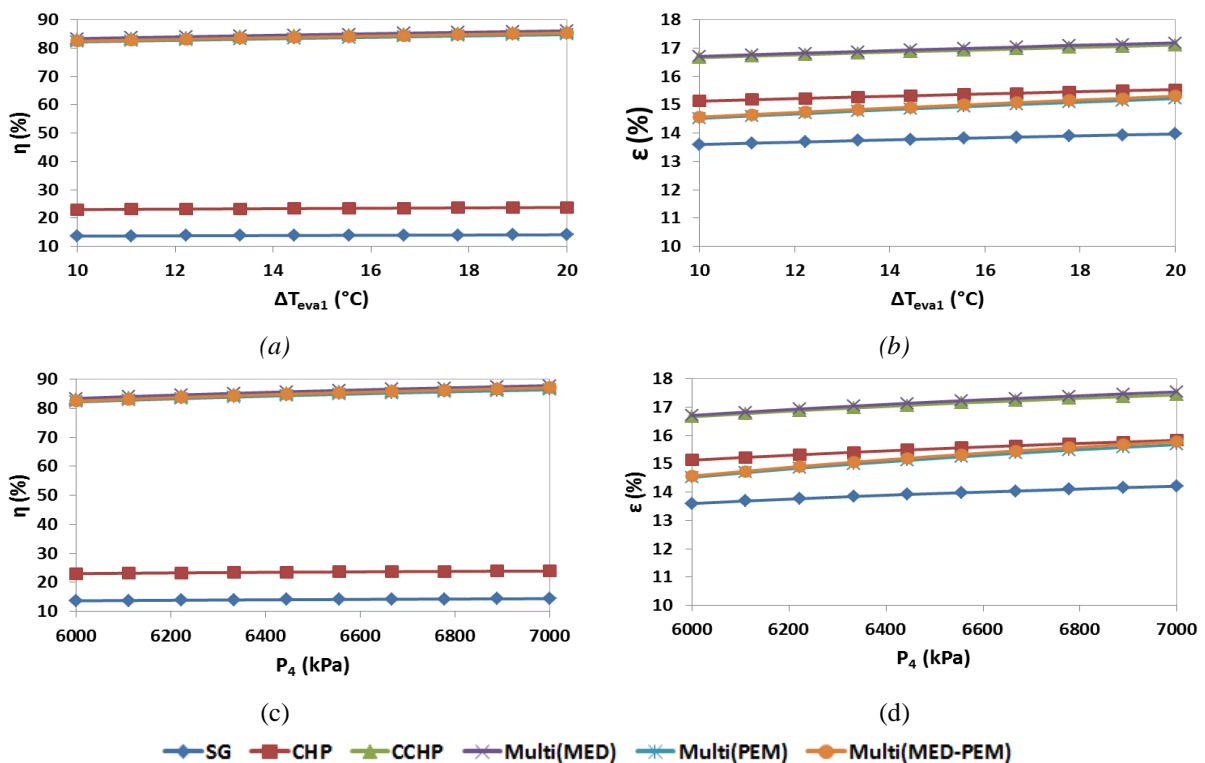


Fig.13. Effects of varying temperature difference of evaporator1 and turbine inlet pressure on thermal and exergy efficiencies of the different cases of multi-generation systems

enhanced, and more electric power is produced. Therefore, the exergy efficiency of all cases increases.

4. Conclusion

In this research paper, a novel multi-generation energy system with solar and biomass as energy inputs to generate useful outputs such as electricity, heating power, cooling power, hydrogen and potable water is suggested for the coastal area of the southern region of Iran. The modeling and investigation of the system are performed based on first and second laws of thermodynamics. The energy and exergy balances are formulated for this system and exergy destruction rates for each component of the system is calculated. Moreover, the impact of increasing outputs on the thermal and exergy efficiencies of the cogeneration systems are discussed in detail. It results that, application of desalination subsystem is more appropriate than integrating electrolyzer as the improvement of exergy efficiency because in MED case, the waste heat of the system is recovered to produce a useful product but in PEM case, high-quality energy (electricity) is converted to less valuable production. The sensitivity analysis is carried out to see the influence of design parameters of the system on overall energy and exergy efficiencies. Therefore, concluding remarks are extracted from the results of the thermodynamic study:

- The thermal and exergy efficiencies of the multi-generation system are found to be 82.5% and 14.6% in the case of that collector aperture area, and the biomass mass flow rate is calculated to be 188,000m² and 6.2ton/h.
- The results of exergy analysis indicate that parabolic trough solar collector, double effect absorption chiller, and biomass combustor destruct 60%, 21%and 8% respectively. Therefore, they are the most inefficient components in comparison to others and in the case of improving the efficiency of the multi-generation system; their performances have the most potential to modify.

The results of parametric study exhibit that, increase in turbine inlet pressure and the temperature difference of evaporator1 lead to an increment in both thermal and exergy efficiencies. While the increase in inlet quality of high-temperature generator and temperature of evaporator2 causes the decrement of exergy

efficiency because the amount of exergy production via cooling output drops down.

References

- [1] Najafi G., et al., Potential of Bioethanol Production from Agricultural Wastes in Iran, *Renewable and Sustainable Energy Reviews*, 13(6-7): 1418-1427 (2009).
- [2] Stackhouse Paul W., Ph.D J., *NASA Surface meteorology and Solar Energy* (2013).
- [3] Ahmadi P., Dincer I., Rosen M.A., Multi-Objective Optimization of an Ocean Thermal Energy Conversion System for Hydrogen Production. *International Journal of Hydrogen Energy*, 40(24): 7601-7608 (2015).
- [4] Taheri M., Mosaffa A., Farshi L.G., Energy, Exergy and Economic Assessments of a Novel Integrated Biomass Based Multigeneration Energy System with Hydrogen Production and LNG Regasification Cycle, *Energy*, 125: 162-177 (2017).
- [5] Akrami E., et al., Energetic and Exergoeconomic Assessment of a Multi-Generation Energy System Based on Indirect Use of Geothermal Energy. *Energy*, 124: 625-639 (2017).
- [6] Sharifishourabi M., Chadegani E.A., Performance Assessment of a New Organic Rankine Cycle Based Multi-Generation System Integrated with a Triple Effect Absorption System. *Energy Conversion and Management*, 150: 787-799 (2017).
- [7] Khanmohammadi S., et al., Exergoeconomic Analysis and Multi Objective Optimization of a Solar Based Integrated Energy System for Hydrogen Production, *International Journal of Hydrogen Energy* (2017).
- [8] Parham K., Alimoradiyan H., Assadi M., Energy, Exergy and Environmental Analysis of a Novel Combined System Producing Power, Water and Hydrogen. *Energy*, 134: 882-892 (2017).
- [9] Boyaghchi F.A., Chavoshi M., Sabeti V., Multi-Generation System Incorporated with PEM Electrolyzer and Dual ORC Based on Biomass Gasification Waste Heat Recovery: Exergetic, Economic and Environmental Impact Optimizations. *Energy*, 145: 38-51 (2018).

- [10]Yuksel Y.E., M. Ozturk, and I. Dincer, Energetic and Exergetic Performance Evaluations of a Geothermal Power Plant Based Integrated System for Hydrogen Production. *International Journal of Hydrogen Energy*, 43(1): 78-90 (2018).
- [11]Bellos E., Tzivanidis C., Multi-Objective Optimization of a Solar Driven Trigeration System. *Energy*, 149: 47-62 (2018).
- [12]FAO, The Future of Food and Agriculture -Trends and Challenges. Rome: Food and Agriculture Organization of the United Nations, 1st Edition (2017).
- [13]Noorpoor A., et al., A Thermodynamic Model for Exergetic Performance and Optimization of a Solar and Biomass-Fuelled Multigeneration System. *Energy Equipment and Systems*, 4 (2): 281-289 (2016).
- [14]Calise F., Figaj R.D., Vanoli L., A Novel Polygeneration System Integrating Photovoltaic/Thermal Collectors, Solar Assisted Heat Pump, Adsorption Chiller and Electrical Energy Storage: Dynamic and Energy-Economic Analysis. *Energy Conversion and Management* (2017).
- [15]Mohammadi A., Mehrpooya M., Energy and Exergy Analyses of a Combined Desalination and CCHP System Driven by Geothermal Energy. *Applied Thermal Engineering*, 116: 685-694 (2017).
- [16]Javidmehr M., Joda F., Mohammadi A., Thermodynamic and Economic Analyses and Optimization of a Multi-Generation System Composed by a Compressed Air Storage, Solar Dish Collector, Micro Gas Turbine, Organic Rankine Cycle, and Desalination System. *Energy Conversion and Management*, 168: 467-481 (2018).
- [17]Rashidi, H. and J. Khorshidi, Xergy analysis and multiobjective optimization of a biomass gasification-based multigeneration system. *Energy Equipment and Systems*, 2018. 6(1): p. 69-87.
- [18]Ghasemi A., Heidarnejad P., Noorpoor A., A Novel Solar-Biomass Based Multi-Generation Energy System Including Water Desalination and Liquefaction of Natural Gas System: Thermodynamic and Thermoeconomic optimization. *Journal of Cleaner Production* (2018).
- [19]Islam S., Dincer I., Yilbas B.S., Development of a Novel Solar-Based Integrated System for Desalination with Heat Recovery, *Applied Thermal Engineering*, 129: 1618-1633 (2018).
- [20]Siddiqui O., Dincer I., Examination of a New Solar-Based Integrated System for Desalination, Electricity Generation and Hydrogen Production. *Solar Energy*, 163: 224-234 (2018).
- [21]Forristall R., Heat Transfer Analysis and Modeling of a Parabolic Trough Solar Receiver Implemented in Engineering Equation Solver. National Renewable Energy Lab., Golden, CO.(US) (2003).
- [22]Boyaghchi F.A., Sabaghian M., Multi Objective Optimisation of a Kalina Power Cycle Integrated with Parabolic Trough Solar Collectors Based on Exergy and Exergoeconomic Concept. *International Journal of Energy Technology and Policy*, 12(2): 154-180 (2016).
- [23]Al-Sulaiman F.A., Exergy Analysis of Parabolic Trough Solar Collectors Integrated with Combined Steam and Organic Rankine Cycles, *Energy Conversion and Management*, 77: 441-449 (2014).
- [24]kalogirou S., *Solar Energy Engineering: Processes and Systems*. UK: Elsevier (2009).
- [25]Miles T.R., et al., Alkali Deposits Found in Biomass Power Plants: A Preliminary Investigation of Their Extent and Nature. National Renewable Energy Lab., Golden, CO (United States); Miles (Thomas R.), Portland, OR (United States); Sandia National Labs., Livermore, CA (United States); Foster Wheeler Development Corp., Livingston, NJ (United States); California Univ., Davis, CA (United States); Bureau of Mines, Albany, OR (United States). Albany Research Center 1 (1995).
- [26]Ni M., Leung M.K., Leung D.Y., Energy and Exergy Analysis of Hydrogen Production by a Proton Exchange Membrane (PEM) Electrolyzer Plant. *Energy Conversion and Management*, 49(10): 2748-2756 (2008).
- [27]Nami H., Akrami E., Ranjbar F., Hydrogen Production Using the Waste Heat of Benchmark Pressurized Molten Carbonate Fuel Cell System via Combination of Organic Rankine Cycle and Proton Exchange Membrane (PEM) Electrolysis. *Applied Thermal Engineering*, 114: 631-638 (2017).

- [28]Gurau V., Barbir F., Liu H., An Analytical Solution of a Half-Cell Model for PEM Fuel Cells. *Journal of the Electrochemical Society*, 147(7): 2468-2477 (2000).
- [29]Chan S., Xia Z., Polarization Effects in Electrolyte/Electrode-Supported Solid Oxide Fuel Cells, *Journal of Applied Electrochemistry*, 32(3): 339-347 (2002).
- [30]Ioroi T., et al., Thin Film Electrocatalyst Layer for Unitized Regenerative PolymerElectrolyte Fuel Cells. *Journal of Power Sources*, 112 (2): 583-587 (2002).
- [31]<http://www.sun.org.ir/>.
- [32]www.fchart.com.
- [33]Frangopoulos C.A., *Exergy, Energy System Analysis and Optimization-Volume III: Artificial Intelligence and Expert Systems in Energy Systems Analysis Sustainability Considerations in the Modeling of Energy Systems*, EOLSS Publications, 3 (2009).